

## **General Disclaimer**

### **One or more of the Following Statements may affect this Document**

- This document has been reproduced from the best copy furnished by the organizational source. It is being released in the interest of making available as much information as possible.
- This document may contain data, which exceeds the sheet parameters. It was furnished in this condition by the organizational source and is the best copy available.
- This document may contain tone-on-tone or color graphs, charts and/or pictures, which have been reproduced in black and white.
- This document is paginated as submitted by the original source.
- Portions of this document are not fully legible due to the historical nature of some of the material. However, it is the best reproduction available from the original submission.

NASA CR-144501

E7.6-10184

CROSS-CORRELATIVE ANALYSIS OF S-193 DATA FOR

TERRAIN CHARACTERISTICS

(FINAL REPORT)

"Made available under NASA sponsorship  
in the interest of early and wide dis-  
semination of Earth Resources Survey  
Program information and without liability  
for any use made thereof."

Dr. H. S. Hayre,

*Project Manager, ERS-1*

WORK DONE UNDER

NASA Contract #NAS 9-13462

August 15, 1975

TR-75-9

TECHNICAL MONITOR

L. York, Mail Code TF6  
P.I. MANAGEMENT OFFICE  
NASA LBJ SPACE CENTER  
HOUSTON, TEXAS 77058

University of Houston  
Wave Propagation Lab.-Electrical Engineering Dept.  
Cullen College of Engineering  
Houston, Texas 77004

(E76-10184) CROSS-CORRELATIVE ANALYSIS OF  
S-193 DATA FOR TERRAIN CHARACTERISTICS  
Final Report (Houston Univ.) 39 p HC \$4.00

N76-18605

CSCL 08B Unclas

G3/43 00184

## List of Figures

<u>NO</u>	<u>Description</u>	<u>Page No.</u>
1	Ground Illumination and Resolution for Pulsed Radar	F-1
2	Transmitted Pulse Shape for S193 Altimeter	F-2
3	Spectral Density of Transmitted Pulse	F-3
4	Topo Quadrangle Map for Oregon	F-4
5	Topo Quadrangle Map for Colorado	F-5

## List of Tables

<u>NO.</u>	<u>TITLE</u>	<u>Page</u>
1	Typical Skylab Data Format	T-1
2	Computer Program for $h(t)$	T-2
3	Power and Phase Angle Spectra Print Out	T-5
4	Useable Skylab Data Dump	T-8
5	Spatial Ground Elevation Topo Data for Records #124 & 125 (Oregon)	T-10
6	Spatial Ground Elevation Topo Data for Records #125 & 125 (Oregon)	T-11
7	Spatial Ground Elevation Topo Data for Records #129 & 131 (Oregon)	T-12
8	Spatial Ground Elevation Topo Data for Records #227 (Colorado)	T-13
9	Spatial Ground Elevation Topo Data for Records Summary	T-14
10	Summary of Calculated Results	T-15

1

### ABSTRACT

Skylab S-193 Altimeter pulse shape data was used to determine the terrain characteristics of the ground illuminated by its transmitted pulse. Certain Skylab passes over the states of Colorado and Oregon were selected in order to include extremely rough, very rough, rolling, and smooth land areas the types of terrain illuminated. These test areas are mostly wooded and the soil moisture content varies considerably from one place to the next. The topographic surface heights data, information about vegetation, and type of terrain etc., was also obtained. In addition, some of the black and white skylab photographs of these areas were used to develop additional general information.

The Skylab Altimeter data for submode (SM), submode ( $SM^2$ ), and sub-submode ( $SM^3$ ), as well as pitch and roll of the spacecraft were examined in order to determine the exact altimeter antenna beam coverage on ground. The latitude and longitude of the altimeter foot-print under lock conditions were translated from special language into simple Fortran IV data using revised computer software. After extensive analysis and examination of all four data tapes supplied, it was established that only tape numbers 906153 and 907259 taken over Oregon and Colorado had technically useful data for this analysis. This pulse shape data was analyzed using special enhanced resolution Fast Fourier Transform programs.

The radar backscatter characteristics of the ground under consideration were approximated by that of a linear system usually characterized by its impulse response. The transmitted pulse shape for the Skylab Altimeter radar system, specified by G.E. calibration tests, was used in this work. The received pulse shape was approximated from bursts of sets of five sample data points of the received in S-193 pulse shape data Mode 1. It was then possible

to obtain the impulse response of the radar illuminated ground surface as a ratio of the Fast Fourier Transform of the received pulse and the transmitted pulse. The resulting frequency domain representation of the said impulse response was cross-correlated with the Fourier Transform of the spatial ground elevation data. The dc-correlation frequency lag was found to be function of the standard deviation, mean slope, as well as the spatial de-correlation distance of the terrain. Usually cross-correlation functions are quite irregular and are not amenable to a simple decorrelation lag analysis, but the said function is shaped somewhat like a  $(\sin x/x)$  function. Its peak occurs at a certain value of lag, and its decreased monotonically to a very low value before it builds up again in somewhat oscillatory mode. This feature was sufficiently regular to enable us to define the decorrelation lag number, as the number of lags at which the cross-correlation function decreases to  $e^{-1}$  times its original maximum value at the specified lag.

Similar results were obtained for relatively flat terrain as well as for very rough, mountainous and wooded areas in both Colorado and Oregon. It was also concluded that it is possible to predict the ground roughness from the S-193 data from empirical relationships derived between the impulse response and various terrain parameters. This concept can be easily implemented in practice, and the practical usefulness of S-193 instrumentation can be phenomenally advanced over that possible with the Skylab Altimeter.

Some of the significant recommendations are:

1. The phase information, normally lost in envelope detection and sampling should have been preserved if the pulse samples were initiated at a prespecified point of the carrier frequency waveform and taken at intervals equal to a twice or an integral multiple of the integral number of its period.

2. The eight return pulse samples should have been taken on each pulse and over its entire width rather than averaging five samples taken over one section of the pulse.

Thus a considerably enhanced spatial resolution could have been achieved by sampling the return pulse at points in time referred to the phase reference of the carrier signal.

## INTRODUCTION

Nine track magnetic tape Skylab Altimeter S-193 data was received from NASA on the following tapes:

1. SL-2 Project No. 8552C Nasa tape #906153 (s19313-101-2-1-73-3)

Covering Oregon Coast      Time: 150-20-35-41  
                                Thru: 150-20-46-45

2. SL-3 Project No. 8550 Nasa tape #907259 (s-93-100-01-12-72A)

Covering Colorado      Time: 215-17-54-13  
                                Thru: 215-18-16-29

3. SL-2 Project No.      Nasa tape #906154/5

Covering the Gulf Coast and Montana  
                                Time: 160-15-03-30  
                                160-15-07-14  
                                160-15-11-35  
                                160-15-18-4

4. SL-3 Project No. 8550 Nasa tape #S193-13-099-01-42-73-B

Covering Mexico and western part of Texas  
                                Time: 258-16-23-06  
                                258-16-45-05  
                                258-16-23-9  
                                258-16-18-4

Since data contained in tape numbers three and four was not associative with preplanned flights and sites for Altimeter Mode 1 overflight, these tapes were not usable in this study. Data from tapes number one and two was taken over the pre-assigned sites, namely sites #851167 and #398295 respectively, and some of this data was for locked position under Mode 1. (see Table I for typical format).

### GROUND TRUTH DATA

The ground truth data including such factors as moisture, rainfall, foliage, season, man-made effects such as timber cuttings, mining or farming, forest fires, etc., type of forestation, crops or grass, etc., and topographical data was collected for both the Oregon and Colorado sites. Furthermore photographic and visual information on landscape, foliage, and crops, etc., was also noted. The topographical maps were also used to obtain spatial elevation data for the ground tracks.

The S-193 Altimeter Node I data over the third pre-assigned Texas Hats Site apparently was not taken during all skylab passes, and therefore the ground truth along the overpass over the planned Hats site was not compiled although topographical maps were available.

### TOPOGRAPHICAL DATA AND ANALYSIS

The spatial resolution of topographical data obtained from topographic maps was 80 feet for all quadrangles for the Colorado site except for the Nucula, Silverton, Wolf Creek, Chama Peak, and Brazos Peak, which had 208 feet resolution. This latter data was interpolated to yield points 80 feet apart, in order to keep the sampled data points uniformly spaced. The spatial resolution for the topographical data for the Oregon site was also 208 feet.

The topo data for each altimeter footprint was recombined to generate eight points, one for each pulse width illuminated area shaped in the form of a circular area for the first pulse width and an annular ring for each of the successive ones for correlation analysis. This is equivalent to a sampling period of the S-193 pulse, so that the path length on the ground illuminated by the altimeter pulse would correspond to the width of the data window. The transmitted pulse illuminates a circular area which spread till its expanse has the depth

(along range) of  $c\tau/2$ , and this area then is said to reflect back the signal received during the time equal to the width of the transmitted pulse (Hayre, 1962). The next composite areas corresponding to annular rings with  $c\tau/2$  radial depth (along the range vector from the transmitter) each are associated with each succeeding intervals of time of equal value to pulse width. (See Fig. 1).

#### GENERAL PULSE SHAPE DATA CHARACTERISTICS

In S-193 pulse shape experiment Mode 1, the consecutive eight samples are so taken that these:

- a. do not belong to the same return pulse
- b. were not consecutive in information sense, except in some "average sense"
- c. could not be said to represent a single footprint of S-193 beam on the ground.

The Skylab Altimeter S-193 Mode 1 pulse data was taken using a pulse train with a nominal pulse width of 100 nanoseconds and a repetition rate of 250 pulses per second. Furthermore, the return pulse was sampled eight times during each pulse duration, and the sample spacing was 25 nanoseconds. This would yield a spatial sample spacing of 84.5 feet for the terrain illuminated by the altimeter beam. Since the Skylab ground speed is approximately 4 miles per second or 21 feet per millisecond, therefore the pulse period is equivalent to  $4 \times 21 = 84$  feet on the ground. The transmitted pulse is stretched in time because the illuminated area on the target changes as the spherical wave front proceeds outwards from the point its leading edge touches the ground until it is completely out of the beam width of the radar as shown in this Figure 1.

### TRANSMITTED PULSE SHAPE

The detailed information on the S-193 transmitted pulse shape was the essential starting point for this analysis, because the ground points effectively influencing the received pulse effected from the ground shall depend on  $Ct/2$  range depth, where  $c$  is the velocity of light or  $3 \times 10^8$  meters/sec and  $t$  is the effective pulse width, which is approximately 72 to 100 nanoseconds.

In Mode I pulse shape S-193 Altimeter experiment, no detailed information on the shape of the transmitted pulse  $x(t)$ , was available in our initial phases and therefore it was assumed to be an ideally square pulse of 13.98ghz carrier. Later on, it was then learned that the pulse shape was indeed somewhat gaussian. The approximate transmitted pulse shape was eventually obtained from the G.E. Calibration Manual obtained from NASA-LBJ Center, and both its time sampled shape and its spectral density are shown in the Figures 2 and 3 which show that it has overshoots in both negative and positive excursions. This stress on the shape of the transmitted pulse is further demonstrated by the Fourier Transforms analysis given below for each of these pulse shapes, since both amplitude and phase spectra of the transmitted pulse are essential for an impulse response analysis.

#### CASE I: Rectangular Pulse

If the envelope of the transmitted pulse  $x(t)$  has a period  $T$  and pulse width  $a$ , then its Fourier Transform pair would be given below:

$$x(t) = \begin{cases} 1 & -a/2 \leq t \leq a/2 \\ 0 & \text{OTHERWISE} \end{cases} \text{ OVER } -T/2 \leq t \leq T/2 \quad (1)$$

$$C_n = \frac{1}{T} \int_{-a/2}^{a/2} x(t) \exp(-j\omega_n t) dt = \left(\frac{a}{T}\right) \frac{\sin(\omega_n a/2)}{(\omega_n a/2)} \quad (2)$$

where  $\omega_n = n\omega_0 = 2\pi n/T$

This results in the following power spectral density  $P_x(f)$

$$P_x(f) = |X(f)|^2 = \sum_{n=-\infty}^{\infty} |C_n|^2 \delta(\omega - \omega_n) \quad (3)$$

and phase angle spectrum:

$$\phi_x(f) = \tan^{-1} (\text{IMAGINARY PART OF } C_n / \text{REAL PART OF } C_n) \quad (4)$$

$= 0$

### CASE II: Gaussian Shape (approximated by $(\sin x/x)$ form)

If the envelope of the transmitted pulse  $x(t)$  is approximated by a gaussian curve, then its Fourier transform pair is given as:

$$x(t) = A (\sin \omega t / \omega t) \quad \text{for } -\infty < t < \infty \quad (5)$$

$$X(f) = \int_{-\infty}^{\infty} x(t) e^{-j2\pi f t} dt \quad (6)$$

$$= \int_{-\infty}^{\infty} A (\sin \omega t / \omega t) \cdot \cos \omega f t dt$$

$$\stackrel{0}{\int} \begin{cases} \frac{\pi}{\omega} & |\omega N| \leq b \\ \frac{\pi}{\omega b} & \omega_N = b \\ 0 & |\omega N| \geq b \end{cases}$$

(7)

Since the following integral holds:

$$\int_{-\infty}^{\infty} (\sin \alpha t \cdot \cos \omega t) / t dt = \begin{cases} \frac{\pi}{\omega} & |\omega| \leq \alpha \\ 0 & \omega = \alpha \\ 0 & \omega > \alpha \end{cases} \quad (8)$$

Note again that the phase spectrum is zero here as well.

### CASE III: Truncated Gaussian Pulse

The real case of S-193 Mode I pulse is closest to a truncated gaussian pulse. For instance, let us say over, one period, one may write  $x(t) = A \exp(-K^2 t^2)$  for  $-T/2 < t < T/2$  and its generalized fourier coefficient  $C_n$  shall be defined as:

$$x(t) = \sum_{n=-\infty}^{\infty} C_n \exp(j\omega_n t) = A \exp(-K^2 t^2) \quad \text{for } -T/2 \leq t \leq T/2 \quad (9)$$

and

$$C_n = \left(\frac{2}{\pi K}\right) \int_{-T/2}^{T/2} \exp(-K^2 t^2 - j\omega_n t) dt \quad (10)$$

Let  $Kt = t_1$ , and therefore  $Kdt = dt_1$ , and hence

$$\begin{aligned} C_n &= \left(\frac{2}{\pi K}\right) \int_0^{Kt_1/2} \exp(-t_1^2) \cos(\omega_n K t_1) dt_1, \\ &= \left(\frac{2}{\pi K}\right) \left(\frac{\sqrt{\pi}}{4K} e^{\omega_n^2 K^2/2}\right) [\operatorname{erf}(x - j\omega_n K/2) + \operatorname{erf}(x + j\omega_n K/2)] \end{aligned} \quad (11)$$

Since

$$\begin{aligned} \int_{-\infty}^{\infty} \exp(-K^2 x^2) \exp(j\omega x) dx &= \\ &= \left[\frac{\sqrt{\pi}}{4} \exp(\omega^2/4)\right] [\operatorname{erf}(x - j\omega/2) + \operatorname{erf}(x + j\omega/2)] \end{aligned} \quad (12)$$

Where

$$\operatorname{erf}(x) = \left(\frac{2}{\sqrt{\pi}}\right) \int_0^x \exp(-t^2) dt \quad (13)$$

Upon substitution of limits one obtains:

$$c_n = (s/Tk) (\pi/16)^{1/2} \exp(wn/2k)^2 \{ \operatorname{erf}(kT/2 - jwn/2k) + \operatorname{erf}(kT/2 + jwn/2k) - 2\operatorname{erf}(jwn/2k) \} \quad (14)$$

$$\text{since } \operatorname{erf}(-x) = \operatorname{erf}(+x) \quad (15)$$

It is important to note that the power spectral density of  $x(t)$  is  $|c_n|^2$ , and its phase spectrum is different from that obtained in cases I and II.

#### CASE IV: Truncated Gaussian Pulse with Fast Drop Off

In this case the Fourier Transform integral for  $c_n$  in the previous case may be modified to extend its upper and lower limits to infinity since the pulse is already assumed to have dropped to negligible or essentially zero amplitude before reaching the limits of its period. Thus one obtains:

$$c_n = (2/\pi) \int_0^\infty \exp(-k^2 \omega^2) \cos \omega t d\omega \quad (16)$$

$$= (2/\pi) (\pi/4k^2)^{1/2} \exp(-\omega^2/4k^2)$$

Note that in this approximation, the power spectral density of  $x(t)$  in a given period is essentially the same as that obtained in Case III but its phase spectrum is zero as was the case in Case I and Case II.

## IMPORTANCE OF POWER SPECTRUM AND PHASE ANGLE SPECTRUM IMPULSE RESPONSE CALCULATIONS

The results obtained above are now shown to have significance in this study, where the power  $P_x(w)$  and phase spectrum  $\phi_x(w)$  of  $X(t)$  are needed to calculate the impulse response of the terrain radiated by S-193 pulse. Let the received pulse  $Y(t)$ , have its power spectral density  $P_y(w)$ , and the phase spectrum  $\phi_y(w)$ . Then the Fourier Transform of  $H(t)$ , the terrain impulse response is given by the following relationships:

$$Y(jw) = X(jw) H(jw) \quad (17)$$

$$P_y(w) = P_x(w) P_h(w) \quad (18)$$

$$\phi_y(w) = \phi_x(w) \cdot \phi_h(w) \quad (19)$$

and therefore

$$H(t) = \frac{1}{2\pi} \int_{-\infty}^{\infty} P_h(w)^{1/2} e^{j\phi_h(w)} e^{-jw\tau} dw = \text{INV F.F.T} \left\{ \left[ \frac{P_y}{P_x} \right] e^{j(\phi_y(w) - \phi_x(w))} \right\} \quad (20)$$

In this connection the Fast Fourier Transform technique (see Program Table 2) is employed to obtain  $h(t)$  from the eight sampled values of  $X(t)$ . A typical program for this effort is attached and it is the result of extensive computer analysis of data samples of the type available from S-193, with basic intent to enhance resolution of the  $h(t)$ .

Early software programs yielded a quick drop-off of the values of  $h(t)$  for  $t$  greater than zero. For instance, the first value, for the data shown in Table 3, was 176.51 and the second value was 0.539. A special technique of padding data with optimum number of zeros was then used to yield at least 4 to 8 point resolution. In this effort eight S-193 return pulse sample values are extended to 256 points by adding 248 zeros at the end, and assuming that the phase angle information for the eight points is unknown and assumed zero as would be the case for envelope detected data. Other programs with assumed phase angle input, using the same eight sample points of  $x(t)$  were also run and the results obtained

were significantly different. Therefore it was concluded that the S-193 system effectiveness would be considerably enhanced if the pulse samples were taken at some specified point of the carrier signal and synchronized with a known starting point on the pulse such as its first positive zero crossing, and thus preserving its phase information.

#### ALTIMETER BEAM FOOT PAD

Since the  $\sim 3\text{db}$  beam width is  $1.6^\circ$ , and its side lobes are 30 db below the level of the main beam, the circular ground area illuminated by first, and the annular rings by the second and third pulse widths of 100 nanoseconds transmitted pulse are generated by the cone angles of  $0 - 0.95^\circ$ ,  $0.95^\circ - 1.35^\circ$ , and  $1.35^\circ - 1.65^\circ$ . Therefore, the  $\sim 3\text{db}$  beam width of  $1.6^\circ$ , for a static case, would only cover approximately 80 - 90% of the third pulse width. Since the beam is traveling at approximately 21 feet per millisecond, the net displacement of the beam for three pulse widths would be  $3 \times 21 \times 100 \times 3/1000 = 18.9$  feet, which would cause negligible stretching of the illuminated area on the ground, i.e. a circle of approximately 35,384' in diameter.

Furthermore, for the pulse repetition rate of 250, the beam travels  $4 \times 21 = 84'$  from the beginning of one transmitted pulse to that of the next. Since only first and third return pulse, for every group of five transmitted, are sampled for the pulse shape (mode 1), the distance traveled by the beam between adjacent sets of samples is 168 ft. and 252 ft. in alternate sampling steps. These distances also represent incremental changes in the ground position of the center of the illuminated area.

#### SAMPLING CYCLE AND DATA

The data in the G. E. Calibration Manual on S-193 shows that the first sample is taken 15 nanoseconds after the digital delay generator is turned on

and is generally in the noise levels. Furthermore, there are 50 frames (1.04 seconds/frame, 260 pulses transmitted and only 104 pulses are received) wherein the first eight samples, 25 nanoseconds apart, during 215 to 425 nanosecond time frame on the received pulse. This lasts for another 61 frames ( $61 \times 104$  pulses received or  $61 \times 260$  pulses transmitted) when the sampling is shifted further to 415 to 615 nanosecond portion of the received pulses for another 61 frames. Then the sampling process reverts back to the above described sampling cycle after 192 frames or  $192 \times 104$  seconds. The above description simply stated shows that the S-193 pulse shape data lacks considerable resolution since one obtains only from the front portion for the first  $15 \times 104$  pulses, and finally another eight points from the tail end of another  $15 \times 104$  pulses.

Since the number of return pulses processed by the altimeter per telemetry frame of 1.04 seconds are 104 whereas the number transmitted is 260. The received pulse is sampled in submodes 0, 1, 2, 3, 4, and 5, etc. for a total of 400 nanoseconds, and yet the beamwidth of 1.60 degrees for vertical incidence, would not allow monitoring of more than 2.8 pulse illuminations on the ground or a period of 280 microseconds which covered by submode (SM) 0 and subsubmodes (SM<sup>2</sup>) 0 as a part of Mode 1.

A complete dump (See Table 4) of Model data for altimeter locked-in position was made with pitch, roll, as SM<sup>2</sup> and SM<sup>3</sup> information, and out of the four tapes received, only tapes #096153 and #907259 for Oregon and Colorado respectively were found to have usable data. Moreover due to loss of lock, there was no data for the following records:

Tape #906153:

121-123, 127, 130, 133-135, 139-149, 150, 155, 157-159, 161, 163, 172, 175-178  
181-187, 189, 191-200, 202-204, 207-211, 213, 215, 217-218, 221, 227-231, 233  
235, 238-241, 245-266, 270, 274, 276-279, 282, 288-304, 306-307.

Tape #907259:

195-200, 205, 208-211, 213-215, 217-220, 222-224, 228-229, 232-244, 250-252,  
255-256, 258-261, 276, 318, 592-598, 601, 610-619, 621-623, 632-653, 656,  
659-663.

The Oregon ground truth data for the flight line from 43-40-36 to 42-28-30  
124-15-0 to 122-15-0 corresponding to S-193 record #124 through #148 (total 25) on tape #90613 was  
processed (see Tables 5, 6, & 7) where records numbered 127, 130, 133, 134, 135,  
139, 140, 141, and 142, (total 9) are not recorded because of loss of lock or  
other such conditions.

Similarly the Colorado ground truth data corresponding to Skylab data on  
tape #907259 covering the flight line from 38-30-30 to 37-19-0 108-54-0 to 106-15-0 and corresponding  
to data records #204 through #232 (total 29) was dumped. Out of these record  
numbers, 205, 208-211, 213-215, 217-220, 222-224, 228-229, and 231 (total 18)  
were missing due to loss of lock etc. The usable data records for Tape #907259  
for Oregon are listed below although only record #227 fell in the region where  
ground truth data (Table 8) was collected:

Records 193, 337, 264, 290, 292, 293, 296, 299,  
301, 304, 306, 307, 309, 312, 312, 316,  
317, 323, 328, 348, 367, 372, 376, 377,  
378, 393, 394, 414, 415, 416, 418, 419,  
420, 427, 436, 437, 439, 441, 442, 450,  
451, 452, 475, 477, 487, 488, 496, 499,  
502, 503, 504, 506, 515, 516, 533, 538,  
543, 550, 554, 555, 559, 560, 562, 581,  
591, 606, 610, 615, 630, 655.

An additional examination of the detailed print-out of these records  
showed that out of the above list total, Mode 1 data as listed on Table 4 con-  
sisted of only nine valid data records as listed in Table 9 in the region of  
interest. Furthermore, only six of these records were processable since the  
topographical data for records #144, 145, and 148 in Oregon was not available.

Therefore, the analysis of this work is based on records #124, 125, 126 and 131 in Oregon and #227 in Colorado.

#### ANALYSIS SUMMARY AND RESULTS

The topographical information obtained along the ground track of the S-193 in Oregon and Colorado, approximately amounts to 14,927 ft, which correspond to either 186 samples taken at 208' or 80' sampling intervals respectively. Moreover, the first eight sampled points from the beginning part of the return pulse correspond to 0,  $6160$ ,  $6160(2)^{1/2}$ ,  $6160(3)^{1/2}$ ,  $6160(4)^{1/2}$ ,  $6160(5)^{1/2}$ ,  $6160(6)^{1/2}$ ,  $6160(7)^{1/2}$  feet on the ground out from the zero point under the nadir.

Since the very steep drop with time in the value of the impulse response in time domain  $h(t)$  from its value at  $t = 0$  does not permit a reliable cross correlation with the topographic data, it was therefore decided to cross correlate the Fourier transform  $H(f)$  of  $h(t)$ , and that of the spatial surface height  $R(r)$  or  $C_{HR}(\Delta f) = \langle H(f) R(f+\Delta f) \rangle$  (21)

One of the easiest and practical elements of this analysis was the use of de-correlation frequency lag of  $C_{HR}(\Delta f)$ . For the sake of simplicity, the de-correlation frequency lag is described as d.c.

The de-correlation frequency of the cross-correlation function between  $R(f)$ , the power spectral density of the surface height  $R(r)$ , and  $H(f)$  the pulse response spectrum for the terrain illuminated by the altimeter beamwidth has been found to be directly related to the roughness of the terrain and its mean elevation. For example an empirical relationship was calculated relating these two variables as given below:

$$\begin{aligned} & \text{de-correlation frequency Shift} \\ & \text{for the Cross Correlation function} \\ & \text{between } R(f) \text{ and } H(f) = \exp. -4.32 R_m, \end{aligned} \quad (22)$$

where  $R_m$  = mean elevation in thousands of feet. All the calculated results were reasonably consistent for all the data records in that these satisfy the above empirical equation. For instance, the said decorrelation frequency decreases from a maximum of 18 at  $R_m$  of 1520 (Record #124) to a minimum of 34 at  $R_m$  of 8850 ft. Similarly, the decorrelation frequency of the spectral density of the surface heights  $R_m(r)$  or  $R_m(t)$ , was found to increase with increase in mean elevation. This variation is inverse to that of the decorrelation of the Cross Correlation function discussed above. An empirical relationship was again derived to approximate this variation and is given below:

decorrelation frequency shift for

the power Spectral density of the

$$\text{Spatial Surface heights} = 1 - \exp[-\beta(R_m + R_o)], \quad (23)$$

where  $\beta = 0.15$  (on the average)

$$R_o = 1.244 \text{ Kiloft.}$$

$R_m$  = measured in Kilofeet.

The above results are significant since one needs no ground based data in order to predict the mean heights as well as slope variation of the terrain illuminated below. For instance,  $d_1 = \text{dcce } R(f)H(f) = \exp. -\alpha R_m$ ,  $d_2 = \text{dc } R(f) = 1 - \exp [-\beta(R_m + R_o)]$ . By differentiating the variable  $R_m$  in terms of  $d_1$  and  $d_2$ , one can positively obtain the slope variation. For instance, from the first equation one obtains:

$$R_m = \ln(d_1/\alpha) \quad (24)$$

$$\text{and } \frac{dR_m}{dd_1} = \frac{-1}{\alpha d_1} \quad (25)$$

and similarly from the second equation, one obtains:

$$1 - d_2 = \exp(-\beta R_m') \quad (26)$$

$$\text{or } R_m^{-1} = -\ln(1-d_2)/\beta \quad (27)$$

$$\text{and } \frac{dR}{dd_2} = 1/(1-d_2)\beta \quad (28)$$

These results were verified in the cases of the six records and the corresponding six sites, where the valid data was available. Similarly, reflectivity was also obtained, utilizing the normalized value of Y in order to determine the ground cover.

### CONCLUSIONS

The impulse response technique, when coupled with fine resolution altimeter data, is capable of yielding,

- a) Very fine mean ground elevation resolution.
- b) Slopes and slope variation along the altimeter path.
- c) The absorption or the ground vegetation cover density for a given weather condition.
- d) An eventual classification of ground cover and/or moisture content of the ground.

It is recommended that the S-193 electronic part of instrumentation be updated at a nominal cost in order to make it an economical tool for earth observation. Its utility would be extremely enhanced if used in a cross correlative mode with optical sensors which are unable to yield the same information as S-193 due to, among other factors, adverse weather conditions. Furthermore S-193 instrumentation package is much less susceptible to roll and pitch variation of the airframe.

### References:

1. Hayre, H. S., Lunar Backscatter Theories -- D.S.C. Dissertation, University of New Mexico, Electrical Engineering Department, Jan. 1962.
2. Grossner W. & N. Hofreiter, Integral Tables Springer-Verlag, Vienna 1961.
3. Skylab Instrumentation Calibration Data Vol. IV (G.E.) NASA-LBJ Space Center, Houston, Texas, Skylab Mission SL-1, Aug. 1973.

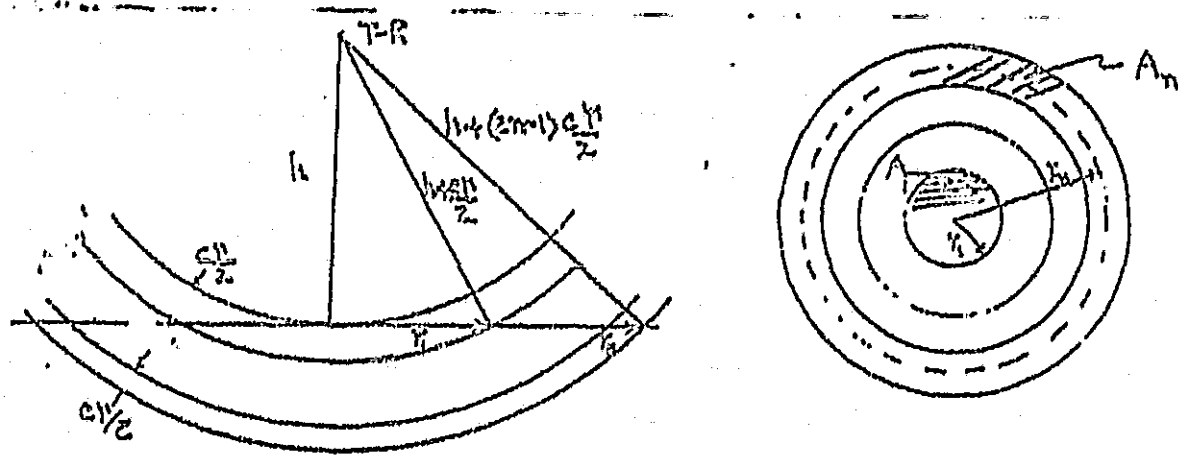
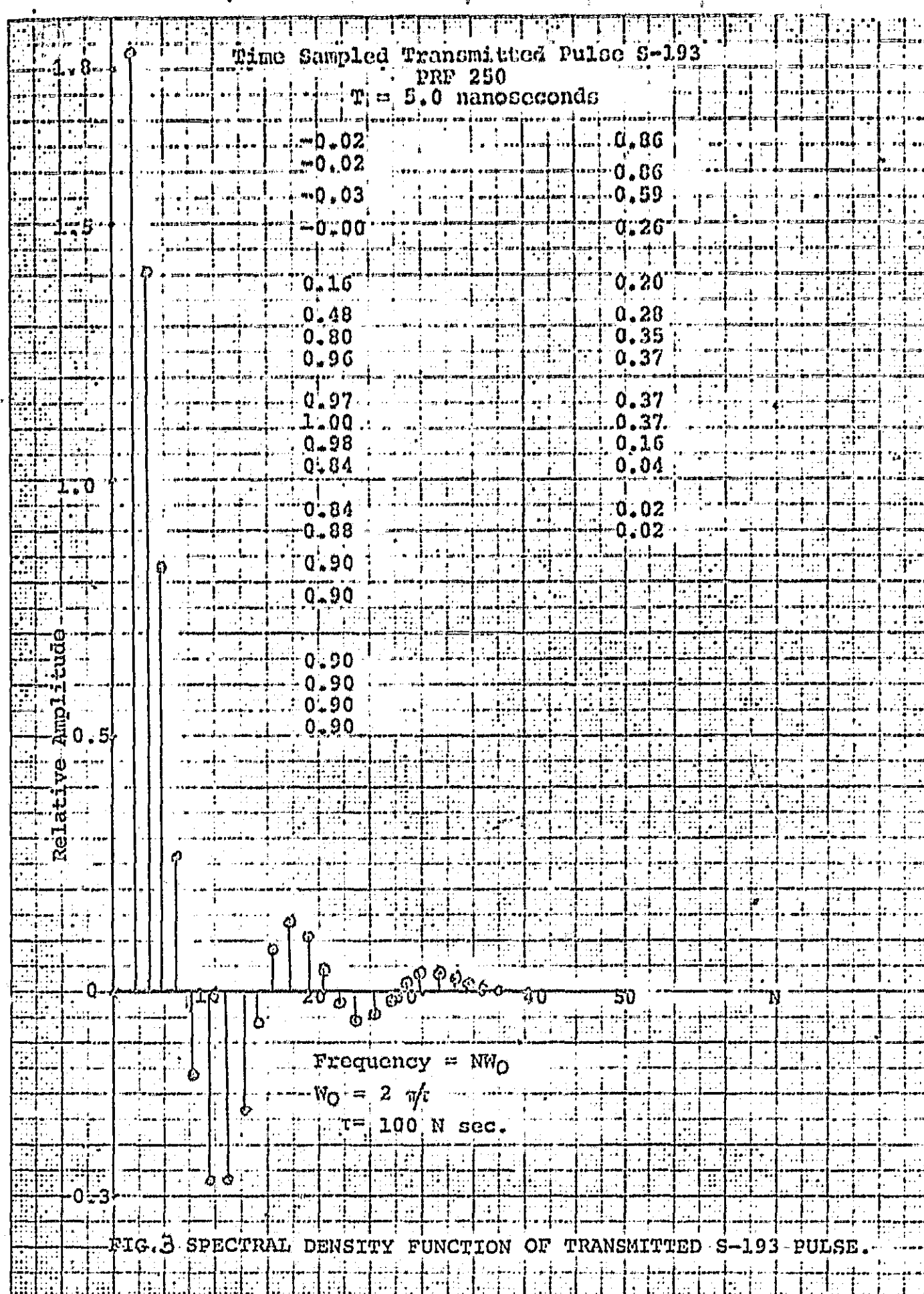


Fig. 1 Consecutive Illuminated Annular Rings on the Ground

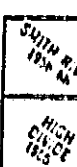
PRECEDING PAGE BLANK NOT FILMED

REPRODUCIBILITY OF THE  
ORIGINAL PAGE IS POOR



## ~~REPRODUCIBILITY OF THE ORIGINAL PAGE IS POOR~~

~~ORIGINAL PAGE IS POOR~~



卷之三

1

2

13

1

8

7

○

四

1

REPRODUCIBILITY OF THE  
ORIGINAL PAGE IS POOR

THE NUMBER OF PUBLISHED MAPS  
SUGGESTED THIS INDEX IS 1254

GREGORY OF NEAR EAST

LASS ACCIUS TO SAM  
AND ALFREDO CALIST  
WANT TO GET IN CANADA  
AS EXCUSES FOR NOT PAYING  
THEIR TAXES.

1936  
Aug 2

LAWRENCE KELLY

卷之三

## ALL ANGLES ARE IN DEGREES

NASA LOGICAL TAPE RECORD NUMBER	TIME	PIECES	FIELD OF VIEW	LAT	LONG	SPACECRAFT GEOMETRIC LAT	PITCH	ROLL
							GIMBAL LONG BIAS	GIMBAL LAT BIAS
906153	109	7427655559	000	43.69	126.06	43.71	125.05	0.77
906153	110	742775953	000	43.67	124.79	43.67	124.97	0.77
906153	111	742786354	000	43.64	124.91	43.64	124.90	0.69
906153	112	742796754	000	43.62	124.82	43.61	124.82	0.68
906153	113	742807154	000	43.59	124.75	43.58	124.76	0.68
906153	114	742817553	000	43.53	124.68	43.55	124.67	0.77
906153	115	742827253	000	43.50	124.60	43.52	124.59	0.69
906153	116	742837353	000	43.47	124.52	43.49	124.51	0.77
906153	117	742847754	000	43.45	124.44	43.46	124.43	0.77
906153	118	742859154	000	43.42	124.37	43.42	124.36	0.58
906153	119	742869554	000	43.38	124.29	43.39	124.28	0.77
906153	120	742879953	000	43.35	124.21	43.36	124.20	0.77
906153	121	742973549	010	43.03	123.53	43.07	123.44	0.77
906153	122	7429994350	010	43.00	123.38	43.01	123.22	0.77
906153	123	7430291550	010	42.93	123.23	42.94	123.14	0.77
906153	124	7430326351	010	42.83	123.00	42.85	122.92	0.77
906153	125	7430396751	010	42.63	122.88	42.64	122.77	0.77
906153	126	7430994350	010	42.43	122.73	42.45	122.64	0.77
906153	127	7431098349	010	42.27	122.55	42.28	122.47	0.77
906153	128	7431191551	010	42.11	122.48	42.11	122.41	0.77
906153	129	7431291551	010	42.03	122.32	42.03	122.24	0.77
906153	130	7431391551	010	41.93	122.16	41.94	122.11	0.77
906153	131	7431491551	010	41.83	122.00	41.85	121.94	0.77
906153	132	7431591551	010	41.73	121.84	41.75	121.77	0.77
906153	133	7431697551	010	41.63	121.68	41.65	121.61	0.77
906153	134	7431791551	010	41.53	121.52	41.55	121.45	0.77
906153	135	7431891551	010	41.43	121.37	41.45	121.32	0.77
906153	136	7431991551	010	41.33	121.22	41.35	121.21	0.77
906153	137	7432097551	010	41.23	121.07	41.25	121.05	0.77
906153	138	7432192550	010	41.13	120.92	41.15	120.87	0.77
906153	139	7432292749	010	41.03	120.77	41.05	120.73	0.77
906153	140	743233549	020	41.24	120.62	41.25	120.59	0.77
906153	141	743254350	020	41.14	120.47	41.15	120.45	0.77
906153	142	743264750	020	41.04	120.32	41.05	120.30	0.77
906153	143	743276149	020	41.07	120.17	41.08	120.14	0.77
906153	144	743285549	020	41.00	120.02	41.02	120.00	0.77
906153	145	743306348	020	41.87	119.87	41.88	119.85	0.77
906153	146	74331202749	020	41.80	119.71	41.81	119.70	0.76
906153	147	74332212749	020	41.73	119.57	41.74	119.56	0.76
906153	148	7433233149	020	41.63	119.42	41.64	119.41	0.76
906153	149	7433254350	020	41.53	119.27	41.54	119.25	0.76
906153	150	7433264750	020	41.43	119.12	41.45	119.11	0.76
906153	151	7433285549	020	41.33	118.97	41.35	118.95	0.76
906153	152	7433295549	020	41.23	118.82	41.25	118.80	0.76
906153	153	7433305549	020	41.13	118.67	41.15	118.65	0.76
906153	154	743336748	020	41.03	118.52	41.05	118.50	0.76
906153	155	7433389547	020	41.00	118.37	41.02	118.35	0.76
906153	156	7433399447	020	41.07	118.22	41.09	118.20	0.76
906153	157	7433410346	020	41.00	118.07	41.02	118.05	0.76
906153	158	7433420748	020	41.59	117.92	41.61	117.89	0.76
906153	159	7433431148	020	41.59	117.78	41.61	117.75	0.76
906153	160	7433441547	020	41.52	117.64	41.54	117.62	0.76
906153	161	7433452350	020	41.49	117.50	41.50	117.48	0.76
906153	162	7433493548	100	41.39	117.35	41.40	117.34	0.76
906153	163	7433566348	100	41.14	117.20	41.15	117.18	0.76
906153	164	7433649547	100	40.96	117.05	40.97	117.03	0.76
906153	165	7433670348	100	40.79	116.90	40.80	116.88	0.76
906153	166	7433784746	100	40.41	116.75	40.42	116.73	0.76
906153	167	7433826347	100	40.24	116.59	40.25	116.57	0.76
906153	168	7433836746	100	39.99	116.52	39.99	116.51	0.76
906153	169	7433891947	100	39.62	116.37	39.63	116.36	0.76
906153	170	7433919946	100	39.34	116.24	39.35	116.23	0.76
906153	171	7433940746	100	39.05	116.10	39.06	116.09	0.76
906153	172	7433971946	100	39.73	115.84	39.74	115.83	0.76
906153	173	7434022346	100	39.70	115.67	39.71	115.66	0.76
906153	174	7434044746	110	39.47	115.57	39.48	115.56	0.77
906153	175	7434107146	110	39.25	115.44	39.26	115.43	0.77
906153	176	7434127946	110	39.17	115.33	39.18	115.42	0.77
906153	177	7434149745	110	39.10	115.50	39.11	115.48	0.77
906153	178	7434159146	110	39.04	115.43	39.07	115.42	0.77
906153	179	7434211145	110	38.87	115.10	38.88	115.09	0.77
906153	180	7434221545	110	38.83	114.97	38.84	114.95	0.77
906153	181	7434471144	110	37.91	114.74	37.92	114.73	0.77
906153	182	7434481544	110	37.87	114.50	37.88	114.50	0.77
906153	183	7434491944	110	37.83	114.34	37.84	114.33	0.77
906153	184	7434512745	110	37.75	114.21	37.76	114.20	0.77
906153	185	7434523145	110	37.71	113.16	37.72	113.13	0.77

ORIGINAL PAGE IS  
OF POOR QUALITY

FOR.US SKYLAP.HA.N.MAIN  
FOR S011-04/04/74-13:47:34 (2,3)

MAIN PROGRAM

STORAGE USED: CODE(1) 000277; DATA(0) 010103; BLANK COMMON(2) 000000

EXTERNAL REFERENCES (BLOCK, NAME)

0003	FOUR1
0004	NINTR\$
0005	NRDUS\$
0006	N101\$
0007	N102\$
0010	NWDUS\$
0011	SQRT
0012	ATAN2
0013	SIN
0014	COS
0015	NSTOP\$

STORAGE ASSIGNMENT (BLOCK, TYPE, RELATIVE LOCATION, NAME)

0000	010020	100F	0000	010022	101F	0000	010032	102F	000
0000	010037	107F	0001	000024	111G	0001	000033	120G	000
0001	000114	155G	0001	000147	170G	0001	000162	177G	000
0000 P	010016	AMEAN	0000 R	007000	ASPECH	0000 R	003000	ASPECY	000
0000 R	000000	DATAY	0000 R	010017	FM	0000 I	010014	I	000
0000 I	010012	NSIG	0000 R	006000	PSPECH	0000 R	002000	PSPECY	000

00100 1\* C\*\*\*\*\*  
00100 2\* C DIMENSION VARIABLES.  
00100 3\* C\*\*\*\*\*  
00101 4\* DIMENSION DATAY(2,512),PSPECY(512),ASPECY(512),  
00101 5\* 1 DATAH(2,512),PSPECH(512),ASPECH(512),  
00101 6\* 2 PTS(8)  
00101 7\* C\*\*\*\*\*  
00101 8\* C ASSIGN FOLLOWING --  
00101 9\* C\*\*\*\*\*  
00103 10\* NPTS = 8.  
00104 11\* NPWR = 512  
00105 12\* NSIG = 256  
00106 13\* CONST = 5.8468  
00106 14\* C\*\*\*\*\*  
00106 15\* C READ IN POINTS.  
00106 16\* C\*\*\*\*\*  
00107 17\* READ (5,100) (PTS(I)),I=1,NPTS  
00115 18\* 100 FORMAT(1F16.3)  
00116 19\* SUM = 0.0  
00117 20\* DO 1 I = 1,NPTS  
00122 21\* SUM = SUM + PTS(I) REPRODUCIBILITY OF THE  
00123 22\* 1 CONTINUE ORIGINAL PAGE IS POOR  
00125 23\* AMEAN = SUM / FLOAT(NPTS).  
00126 24\* WRITE(6,101)  
00130 25\* 101 FORMAT (' THE FOLLOWING POINTS - MEAN WERE READ: ')  
00131 26\* DO 2 I = 1,NPTS  
00134 27\* PTS(I) = PTS(I) - AMEAN

T-3

## REPRODUCIBILITY OF THE ORIGINAL PAGE IS POOR

END OF COMPILATION:

## NO DIAGNOSTICS.

QMAP,IN .MAP,.ABS  
MAP 0023-04/04-13:47 -(,0)

T-4

QXOT .ABS

THE FOLLOWING POINTS - MEAN WERE READ:

POINT( 1)=	.450
POINT( 2)=	.268
POINT( 3)=	.120
POINT( 4)=	-.001
POINT( 5)=	-.101
POINT( 6)=	-.182
POINT( 7)=	-.249
POINT( 8)=	-.304

SPECTRA OF INVERSE DATA H.

FREQUENCY	POWER SPECTRA	ANGLE SPECTRA				
1	176.151	-.001	62	.676	1.525	
2	104.049	-.001	63	.637	1.458	
3	46.866	-.001	64	.614	1.374	
4	.539	-.3.135	65	.609	1.270	
5	39.716	3.141	66	.631	1.145	
6	71.451	3.141	67	.692	1.006	
7	97.701	3.141	68	.821	.858	
8	119.250	3.141	69	1.078	.713	
9	.173	2.198	71	1.627	.508	
10	.200	2.114	72	3.165	.486	
11	.231	2.050	73	26.921	.392	
12	.264	2.000	74	11.340	.407	
13	.301	1.960	75	1.523	.553	
14	.341	1.927	76	5.407	-2.803	
15	.386	1.901	77	10.330	-2.781	
16	.435	1.879	78	13.604	-2.774	
17	.491	1.860	79	15.481	-2.772	
18	.553	1.845	80	15.470	-2.772	
19	.624	1.832	81	3.193	.433	
20	.706	1.821	82	1.530	.495	
21	.801	1.811	83	.967	.558	
22	.911	1.803	84	.687	.620	
23	1.042	1.796	85	.523	.685	
24	1.198	1.790	86	.418	.752	
25	1.388	1.785	87	.346	.818	
26	1.623	1.781	88	.294	.886	
27	1.917	1.777	89	.257	.953	
28	2.295	1.774	90	.228	1.019	
29	2.793	1.771	91	.206	1.085	
30	3.470	1.769	92	.189	1.150	
31	4.428	1.767	93	.177	1.215	
32	5.860	1.766	94	.167	1.280	
33	8.171	1.764	95	.160	1.345	
34	12.369	1.764	96	.156	1.411	
35	21.887	1.763	97	.154	1.478	
36	62.372	1.761	98	.155	1.545	
37	44.452	-.1.380	99	.159	1.614	
38	64.118	-.1.380	100	.166	1.683	
39	64.698	-.1.379	101	.179	1.750	
40	56.437	-.1.379	102	.199	1.817	
41	42.295	-.1.379	103	.229	1.882	
42	23.350	-.1.379	104	.277	1.942	
43	3.321	1.764	105	.356	1.997	
44	59.536	1.761	106	.500	2.047	
45	19.782	1.762	107	.818	2.088	
46	11.325	1.762	108	2.005	2.118	
47	7.582	1.761	109	2.930	-.985	
48	5.503	1.760	110	3.181	-.985	
49	4.201	1.758	111	2.732	-.983	
50	3.323	1.755	112	2.017	-.979	
51	2.700	1.752	113	1.147	-.967	
52	2.241	1.747	114	.165	-.805	
53	1.891	1.741	115	1.041	2.116	
54	1.619	1.734	116	3.067	2.134	
55	1.403	1.724	117	.861	2.116	
56	1.229	1.712	118	.494	2.095	
57	1.087	1.696	119	.339	2.072	
58	.970	1.676	120	.254	2.052	
59	.873	1.651	121	.201	2.031	
60	.793	1.618	122	.166	2.011	
61	.728	1.577	123	.140	1.992	
				.122	1.973	

124	.107	1.955	186	.052	2.420
125	.096	1.938	187	.019	2.251
126	.087	1.922	188	.019	2.191
127	.079	1.905	189	.014	2.163
128	.073	1.889	190	.013	2.150
129	.068	1.872	191	.012	2.144
130	.064	1.855	192	.012	2.142
131	.060	1.835	193	.011	2.143
132	.057	1.814	194	.011	2.147
133	.054	1.789	195	.011	2.152
134	.052	1.760	196	.010	2.158
135	.051	1.724	197	.010	2.164
136	.050	1.679	198	.010	2.171
137	.050	1.622	199	.010	2.178
138	.051	1.548	200	.010	2.186
139	.055	1.453	201	.009	2.194
140	.062	1.330	202	.009	2.202
141	.080	1.181	203	.009	2.210
142	.130	1.010	204	.009	2.217
143	.566	.815	205	.009	2.225
144	.136	.979	206	.009	2.233
145	.087	-2.702	207	.009	2.240
146	.211	-2.503	208	.008	2.246
147	.283	-2.467	209	.008	2.251
148	.314	-2.456	210	.008	2.253
149	.307	-2.455	211	.008	2.250
150	.247	-2.474	212	.008	2.237
151	.157	.905	213	.008	2.191
152	.077	1.057	214	.010	1.931
153	.053	1.186	215	.008	2.359
154	.042	1.295	216	.007	2.589
155	.036	1.387	217	.007	2.710
156	.031	1.465	218	.007	2.762
157	.028	1.530	219	.007	2.761
158	.026	1.584	220	.007	2.712
159	.025	1.630	221	.007	2.592
160	.023	1.670	222	.008	2.178
161	.022	1.704	223	.007	2.322
162	.021	1.734	224	.007	2.373
163	.021	1.761	225	.007	2.404
164	.020	1.785	226	.007	2.427
165	.019	1.807	227	.007	2.447
166	.019	1.828	228	.007	2.463
167	.018	1.847	229	.007	2.483
168	.018	1.866	230	.006	2.498
169	.017	1.884	231	.006	2.513
170	.017	1.902	232	.006	2.527
171	.017	1.920	233	.006	2.541
172	.017	1.940	234	.006	2.554
173	.016	1.962	235	.006	2.567
174	.016	1.987	236	.006	2.579
175	.017	2.019	237	.006	2.594
176	.017	2.063	238	.006	2.608
177	.019	2.128	239	.006	2.622
178	.027	2.249	240	.006	2.635
179	.037	-.430	241	.006	2.649
180	.031	-.398	242	.006	2.663
181	.020	-.287	243	.006	2.677
182	.009	.142	244	.006	2.691
183	.009	1.750	245	.006	2.705
184	.020	2.229	246	.006	2.719
185	.033	2.357	247	.006	2.733

248	.006	2.747
249	.006	2.761
250	.005	2.767
251	.005	2.784
252	.006	2.800
253	.006	2.816
254	.006	2.832
255	.006	2.846
256	.006	2.861

NASA TAPE	LOGICAL RECORD NUMBER	TIME	FIELD OF VIEW		SPACECRAFT GEODETIC		MODES
			LAT	LONG	LAT	LONG	
906153	124	742973549	43.06	123.53	43.07	123.52	010
"	125	742983951	43.03	123.46	43.04	123.44	010
"	126	742994350	43.00	123.38	43.01	123.37	"
"	129	743025550	42.90	123.15	42.91	123.14	"
"	131	743046351	42.83	123.00	42.85	122.99	"
"	144	743181551	42.40	122.03	42.42	122.02	"
"	145	743191950	42.39	121.96	42.39	121.95	"
"	148	743223149	42.30	121.74	42.29	121.73	"
"	232	744107146	39.25	115.77	39.26	115.75	110
"	244	744231945	38.79	114.97	38.80	114.95	"
"	271	744512745	37.75	113.21	37.76	113.20	"
"	272	744523145	37.71	113.15	37.72	113.13	"
907259	193	649617683	38.75	109.38	38.76	109.37	000
"	227	649971277	37.43	107.22	37.51	107.29	010
"	264	650408076	35.70	104.64	35.74	104.56	020
"	290	650688878	34.61	102.94	34.61	102.94	110
"	292	650709678	34.51	102.84	34.53	102.82	"
"	293	650720076	34.48	102.77	34.48	102.77	"
"	296	650751277	34.35	102.58	34.36	102.59	"
"	299	650782477	34.23	102.42	34.23	102.41	"
"	301	650803276	34.13	102.30	34.15	102.30	"
"	304	650834476	34.01	102.13	34.02	102.12	"
"	306	650855276	33.92	102.01	33.93	102.01	"
"	307	650865677	33.89	101.96	33.89	101.95	"
"	309	650886477	33.80	101.83	33.80	101.78	"
"	312	650917675	33.67	101.67	33.68	101.66	120
"	313	650928076	33.63	101.62	33.63	101.60	"
"	314	650938476	33.59	101.55	33.59	101.55	"
"	316	650959276	33.49	101.43	33.50	101.43	"
"	317	650969676	33.47	101.38	33.46	101.37	"
"	323	651032075	33.19	101.03	33.20	101.03	"
"	328	651084076	32.98	100.74	32.99	100.75	"
"	348	651344076	31.87	999384	31.89	999385	210
"	368	651805E3E	20.04	98.9E	20.06	98.9E	010
"	372	651847130	29.72	986880	29.78	986880	"
"	376	651888730	29.54	96.55	29.55	966584	"
"	377	651899131	29.50	986409	29.51	986409	"
"	378	651909531	29.45	986444	29.46	986483	"
"	393	652065531	28.76	95.66	28.78	95.66	020
"	394	652075931	28.71	95.61	28.73	95.60	"
"	414	652304726	27.71	94.49	27.71	94.48	110
"	415	652315126	27.66	94.43	27.67	94.43	"
"	416	652325526	27.61	94.39	27.62	94.38	"
"	418	652346326	27.53	94.29	27.53	94.28	"
"	419	652356726	27.48	94.24	27.48	94.23	"
"	420	652367127	27.43	94.18	27.44	94.18	"
"	427	652439928	27.09	93.83	27.11	93.83	"
"	436	652533527	26.69	93.39	26.69	93.39	120
"	437	652543927	26662	93.34	26.64	93.34	"
"	439	652564726	26.53	993223	26.55	93.24	"
"	441	652585528	26.45	993.14	26.46	93.14	"
"	442	652595926	26.40	93.09	26.41	93.09	"
"	450	652679127	26.03	92.70	26.03	92.80	"
"	451	652689526	25.98	92.66	25.99	92.65	"
"	452	652699926	25.93	92.60	25.94	992680	"

"	475	653022324	24.44	91.10	24.47	91.11	210
"	477	653043125	24.34	90.99	24.37	91.01	"
"	487	653147124	23.86	90.52	23.89	90.54	"
"	488	653157524	23.82	90.49	23.84	90.50	220
"	496	653240723	23.44	90.10	23.46	900112	"
"	499	653271924	23.29	89.97	23.32	89.98	"
"	502	653303124	23.13	89.83	23.17	89.84	"
"	503	653313524	23.10	89.77	23.12	889779	"
"	504	653323922	23.04	89.73	23.07	89.75	"
"	506	653344723	22.95	89.65	22.98	89.66	"
"	515	653459122	22.43	89.15	22.45	889.15	410
"	516	653469523	22.38	89.10	22.40	89.10	"
"	533	655681726	11.73	799908	11.80	79.98	010
"	538	655733725	11.49	79.78	11.54	79.77	"
"	543	655785726	11.29	79.58	11.29	79.57	"
"	550	655858527	10.91	79.28	10.93	79.29	020
"	554	655900126	10.73	79.12	10.72	79.13	"
"	555	655910526	10.67	79.07	10.67	79.09	"
"	559	655952127	10.47	78.92	10.47	78.92	"
"	560	655962527	10.41	78.88	10.42	78.89	"
"	562	655983327	10.31	78.79	10.32	78.81	"
"	581	656222525	9.12	77.88	9.14	77.89	110
"	582	656232925	99.08	77.85	9.09	77.85	"
"	583	656243325	9.02	77.80	9.02	77.81	"
"	584	656253725	8.98	77.77	8.99	77.77	"
"	586	656274525	8.88	77.69	8.88	77.69	"
"	587	656284925	8.82	77.64	8.83	77.65	"
"	591	656326524	8.61	77.50	8.63	77.49	"
"	606	656482316	7.84	76.90	7.86	76.90	"
"	610	656565717	7.43	76.59	7.45	76.58	120
"	615	656617716	7.17	76.39	7.19	76.38	"
"	630	656773716	6.40	75.79	6.42	75.79	"
"	655	657022717	5.11	74.81	5.13	74.82	"

## CAMAVALLEY

ORE. Record #  
124 & 125

880	1040	1500	1760	1680
880	960	1520	1680	1680
880	960	1520	1600	1600
880	960	1520	1520	1600
880	960	1520	1440	1610
880	880	1520	1420	1680
800	880	1500	1400	1760
810	920	1480	1380	1800
830	960	1480	1380	1840
840	900	1480	1360	1840
860	880	1520	1360	1880
880	880	1520	1360	1920
880	840	1520	1760	2000
880	800	1520	1760	2025
870	776	1520	1760	2000
870	776	1520	1760	1920
860	740	1520	1760	1840
860	720	1600	1760	1760
850	700	1600	1760	1700
840	720	1600	1760	1670
830	800	1600	1760	1600
810	800	1600	1760	1520
800	880	1600	1760	1440
800	960	1600	1740	1360
880	1040	1600	1720	1320
880	1120	1600	1680	1200
890	1200	1600	1640	1200
920	1120	1600	1680	1120
940	1080	1600	1680	1080
960	1120	1620	1600	1040
960	1200	1640	1600	1000
1000	1120	1680	1620	920
1040	1040	1680	1620	880
1120	1040	1680	1610	880
1200	1120	1680	1605	820
1200	1200	1760	1600	
1200	1280	1760	1610	
1120	1360	1760	1680	
1120	1440	1760	1680	
1090	1480	1760	1680	

ROSEBURG, ORE.  
Record #125&126

840	1460	2000	1760	720
880	1460	2080	1680	720
960	1500	2160	1720	720
1040	1540	2160	1720	720
1110	1580	2000	1680	740
1140	1600	2040	1600	760
1160	1600	2040	1520	780
1120	1600	2080	1520	780
1120	1520	2120	1520	780
1120	1520	2180	1440	
1120	1600	2160	1200	
1120	1600	2120	1040	
1120	1600	2080	960	
1200	1680	2040	920	
1280	1620	2020	800	
1280	1560	2000	760	
1280	1520	1960	720	
1200	1440	1960	660	
1160	1400	1920	660	
1080	1400	1880	660	
1000	1400	1880	660	
1080	1360	1880	720	
1120	1360	1840	720	
1160	1440	1800	660	
1180	1500	1760	660	
1200	1520	1720	660	
1200	1520	1680	660	
1280	1520	1600	660	
1360	1520	1520	660	
1480	1600	1440	660	
				660
1500	1560	1400	660	660
1500	1520	1440	720	660
1420	1560	1440	720	660
1300	1600	1520	720	660
1280	1640	1600	720	
1280	1680	1680	720	
1280	1760	1680	720	
1320	1800	1760	720	
1360	1880	1880	720	
1380	1960	1800	720	

DAYS CREEK, ORE.  
Record #129

## ELEVATION (FT)

2160	1780	1440	2400	2400	2080	2960	3680
2240	1760	1600	2560	2560	2160	2960	3720
2240	1600	1760	2640	2640	2200	3000	3680
2160	1680	1760	2720	2640	2200	2960	3640
2080	1760	1760	2760	2560	2160	2960	3640
1920	2000	1760	2760	2400	2080	2960	
1840	2160	1600	2720	2280	2080	2960	
1680	2280	1600	2560	2280	2160	3040	
1600	2160	1600	2400	2320	2200	3120	
1520	2000	1600	2320	2400	2260	3280	
1440	1920	1600	2320	2480	2400	3320	
1520	1840	1600	2400	2640	2480	3320	
1580	1760	1680	2480	2800	2560	3320	
1520	1760	1760	2640	2880	2600	3280	
1440	1840	1760	2800	2920	2600	3240	
1360	1840	1760	2880	2880	2560	3200	
1240	1920	1680	2880	2780	2480	3200	
1240	1840	1600	2880	2780	2560	3160	
1360	2000	1680	2800	2880	2640	3120	
1360	2000	1840	2640	2960	2720	3240	
1360	2000	1920	2480	2960	2840	3240	
1360	2000	2000	2400	2880	2800	3120	
1360	2000	2080	2320	2720	2640	3200	
1360	1840	2160	2160	2560	2560	3280	
1440	1760	2080	2080	2480	2400	3340	
1520	1600	2000	2000	2400	2360	3340	
1600	1440	2080	1920	2320	2360	3280	
1680	1440	2080	1840	2240	2320	3240	
1760	1440	2000	1840	2240	2320	3240	
1920	1440	1920	1720	2240	2320	3240	
2080	1360	1820	1760	2220	2240	3280	
2120	1280	2000	1840	2200	2120	3360	
2080	1200	2080	1840	2180	2160	3440	
2000	1200	2160	1840	2160	2200	3520	
1840	1200	2320	1880	2080	2200	3600	
1720	1200	2400	1920	2000	2240	3680	
1600	1200	2480	2080	2000	2400	3760	
1680	1200	2560	2240	2080	2480	3760	
1840	1200	2480		2240	2560	3720	
2000	1200	2400		2200	2640	3680	
2080	1200	2320		2160	2720	3600	
2240	1280	2240		2000	2800	3520	
2240	1280	2080		1920	2880	3460	
2080	1280	2240		1960	2880	3520	
1940	1360	2320		2040	2960	3640	

BEAR MOUNTAIN, COLO. & OAKBUSH RIDGE, COLO.  
Record #227

ELEVATION (FT)

8480	8600	7640
8400	8600	7760
8600	8600	7760
8720	8600	7760
8600	8600	7760
8520	8600	7760
8560	8600	7760
8600	8560	7760
8600	8480	7760
8600	8360	7760
8520	8360	7760
8480	8280	7760
8240	8200	7760
8050	8200	7760
7960	8280	7760
7960	8360	7800
8120	8360	7840
8280	8360	7840
8400	8320	7840
8460	8320	7840
8460	8280	7840
8360	8080	7880
8400	7840	7880
8280	7680	7920
8160	7680	7920
8040	7720	7920
7920	8000	7920
7760	7900	7920
7800	7880	
7890	7840	
8000	7760	
8120	7640	
8200	8680	
8360	7760	
8560	7640	

## SKYLAB DUMP DATA

	RECORD	NASA #	LAT	LONG	NAME OF QUADRANGLE
Oregon	124	906153	43.06 3.6'	123.53 31.8'	Camas, Ore Rosenberg
	125	"	43.03 1.8"	123.46 27.6'	Rosenberg, Ore Camas
	126	"	43.00 0'	123.38 22.8'	Rosenberg, Ore Canyonville
	129	"	42.90 54'	123.15 9'	Days Creek, Ore
	131	"	42.83 49.8'	123.00 0'	Days Creek, Ore Tiller
	144	"	42.40 24'	122.03 1.8'	Lake of Woods, Ore
	145	"	42.39 23.4'	121.96 57.6'	Modoc, Ore
	148	"	42.30 18'	121.74 44.4'	Swan Lake, Ore
Colorado	227	907259	37.43 25.8'	107.22 13.2'	Bear Mt, Colo Oakbrush

PARAMETER	X_n	1.0000	1.0000	1.0000	1.0000
$\gamma_n$	1520.5	1808.0	1770.2	2235.0	3480.7
$\gamma_m$	381.00	387.00	381.00	387.00	373.00
$m_R$	.52663-01	.73262-01	.15038	.92500-01	.93775-01
SDR	.37010-01	.71378-01	.97454-01	.43802-01	.60923-01
dCH(Σ)	.63321206	.63321206	.63321206	.63321206	.63321206
dCR(t)	-6321206	.6321206	-6321206	-6321206	1.352745
dCR(£)	15.09422	17.01093	21.02088	21.09551	33.04630
dcCCR(£)H(£)	218.00443	49.03038	68.01351	19.00000	23.50000